IGHEM - International Group for Hydraulic Efficiency Measurement
RENO 1998

Integration Error of Multipath Acoustic Discharge Measurements in Closed Conduits

Alexandre Voser, T. Staubli

Abstract

One of the more important measuring uncertainties of multi-chordal acoustic flow meters arises from integration of the path velocities to evaluate the discharge. In general, this uncertainty may be reduced by employing OWICS (Optimal Weighted Integration for Circular Sections), which is based on an analytical optimization of the integration for ideally turbulent flows. The presented paper focuses on numerical simulation calculations to quantify the integration errors of disturbed velocity distributions. On one hand, disturbed velocity profiles were computed using a CFD-code and, on the other hand, experimental data of probe- and LDA-measurements were used. For both ways, path velocities were numerically simulated and a simulated acoustic discharge reading was compared with the integrated volume flux. The difference yields to the integration error, which was evaluated for various flow configurations, such as flows behind bends and valves as a function of the mounting angle. The results of the integration error analysis evidently show that the uncertainty of an eight path acoustic meter will not exceed ±1% even for heavily disturbed flow within short distances behind the disturbing element. For measuring cross-sections 5D downstream from a disturbing element, the error is estimated to be smaller than ±0.5 % for Reynolds numbers below 10^6 and smaller than ±1% for very large Reynolds numbers. To achieve these integration errors, ideal mounting angles for each investigated disturbing element will be given.

1. Introduction

Regardless of the number of acoustic paths installed, an acoustic flowmeter will never be provide full information on the flow field. Because the discharge calculation of the **A**coustic **D**ischarge **M**easurement (ADM) is based on numerical integration in form of a weighted summation, the missing information results in a measurement error usually called integration error. With a known axial flow field U(x,y), it can be explained by comparing the reference flow function

$$F_{ref}(y) = \int_{-\sqrt{R-y^2}}^{+\sqrt{R-y^2}} U(x,y)\,dx \ ,$$

to the interpolating polynom $F_{ipol}(y)$ of fourth order (for a flowmeter with 4 acoustic elevation planes), which is determined using the “measured” mean velocities multiplied with the projected path lengths. The shape of this polynom is closely linked to the integration method chosen. According to Figure 1, the absolute value of the integration error E_{ADM} can then be represented by the area between F_{ref} and F_{ipol}, or expressed mathematically by

$$E_{ADM} = Q_{ref} - Q_{ADM} = \int_{-R}^{R} F_{ref}(y) - F_{ipol}(y)\,dy$$

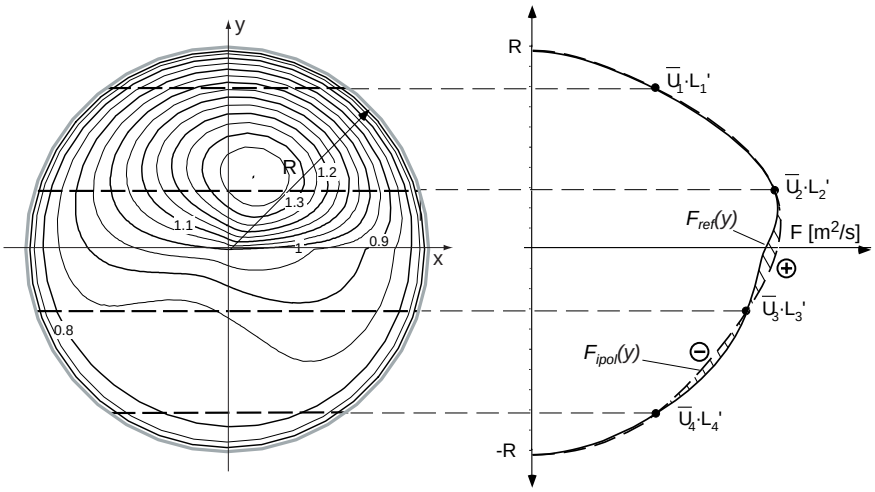

Fig.1 *Illustration of the integration error for a theoretical axial velocity distribution. The interpolating polynom F_{ipol} has been computed using the Gauss-Jacobi integration method [IEC41, 1991].*

Integration errors can be separated in two categories: Integration errors of fully developed, turbulent profiles, the ideal case, and of disturbed profiles. While the main focus of this paper will be on disturbed profiles, the progresses reported at the 96’ IGHEM seminar [STA96] with fully developed profiles will briefly be recapitulated in the following chapter.

2. Integration error of fully developed, turbulent flow profiles

To reduce the Reynolds number dependent error of fully developed, turbulent flow profiles, we propose the integration method called OWICS (**O**ptimal **W**eighted **I**ntegration for **C**ircular **S**ections) which reduces the error by +0.1% to +0.2%. In

contrast to the Gauss-Jacobi method, the weights are calculated individually from actually measured transducer positions:

$$W_1 = \frac{g_1 D^2 (d_3 + d_4 - d_2) - g_2 d_2 d_3 d_4}{\left(1 - 4d_1^2/D^2\right)^{\kappa} (d_1 - d_2)(d_1 + d_3)(d_1 + d_4)}$$

$$W_2 = \frac{g_1 D^2 (d_3 + d_4 - d_1) - g_2 d_1 d_3 d_4}{\left(1 - 4d_2^2/D^2\right)^{\kappa} (d_2 - d_1)(d_2 + d_3)(d_2 + d_4)}$$

$$W_3 = \frac{g_1 D^2 (d_1 + d_2 - d_4) - g_2 d_1 d_2 d_4}{\left(1 - 4d_3^2/D^2\right)^{\kappa} (d_3 - d_4)(d_1 + d_3)(d_2 + d_3)}$$

$$W_4 = \frac{g_1 D^2 (d_1 + d_2 - d_3) - g_2 d_1 d_2 d_3}{\left(1 - 4d_4^2/D^2\right)^{\kappa} (d_4 - d_3)(d_1 + d_4)(d_2 + d_4)}$$

The constants have been fine-tuned for the same positioning of the acoustic paths than those prescribed for the Gauss-Jacobi Method, i.e. $d_1/R = -d_4/R = 0.809017$ and $d_2/R = -d_3/R = 0.309017$. The values for the constants are $g_1 = 0.0900812$, $g_2 = 1.5133647$ and $\kappa = 0.6$ which results in weights $W_1 = W_4 = 0.365222$ and $W_2 = W_3 = 0.598640$ for the distances d_i/R listed above. The discharge is then obtained using the summation formulae described in the IEC Code 41 [IEC41, 1991].

3. Integration errors for disturbed flow profiles

While the integration error for undisturbed flow is well understood, there is little knowledge on the errors of disturbed flow profiles. This is also expressed by the total error estimate of 1% - 2% listed in the IEC41 code, with the integration error being the largest part of it. While an overall error of 1% is considered as good for a primary measurement method, an error of 2% would be less than satisfactory. Several results from comparative measurements indicate however, that the integration error of an 8-path flowmeter is much closer to ±1% than to 2%, even when the measuring section is located directly behind one or more bends [GRE87, MAN95]. Laboratory measurements from BRUTTIN [BRU97] (see Figure 2) give an additional indication that integration errors are lower than often thought: If the systematic error of +0.16% equal to the mean error is deduced, no measurement error, including those for “bad” mounting angles, exceeded the range of ±1%.
To confirm these observations, integration errors related to a selection of very common piping elements, namely single bends, double bends and valves have been investigated by means of numerical simulation calculations based on experimentally determined flow profiles.

3.1 Reduction of the integration error with OWICS

Because disturbed flow profiles can be viewed as superposition of a fully developed flow profile with a disturbance part, all types of flow profiles should benefit from OWICS. This is supported by comparative measurements conducted at the IMHEF Laboratory in Lausanne, where the integration error of the ADM was evaluated behind different bends, convergent pipe elements, a swirl generator and a cylindrical bar [BRU97].

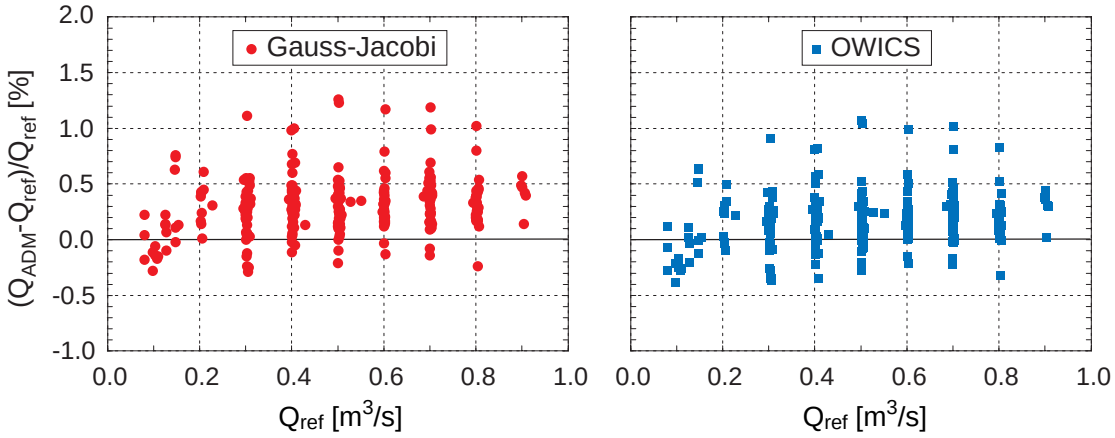

Fig.2 *The Gauss-Jacobi integration method in comparison to OWICS: Measurement errors of all comparative measurements conducted at the IMHEF Laboratory in Lausanne behind disturbing elements. The upstream distances to the disturbing element were 1D, 6D and 11D (Source of data: BRUTTIN [BRU97]).*

Using OWICS, the mean error of all measurements is +0.16% versus +0.32% with the Gauss-Jacobi method, while the error range is nearly unchanged (1.5% versus 1.6%).
Because of these positive results, OWICS was used exclusively for all numerical simulation calculations in this chapter.

3.2 Methods to investigate integration errors of distorted flow profiles

Not each method is equally suited for assessing integration errors. To estimate the results correctly, it is important to know the advantages and disadvantages of the individual methods:

- Comparative laboratory measurements. Because hydraulic laboratories are very often equipped with very precise volumetric calibration devices, the total error of the ADM can be measured with a high accuracy. However, the individual contributions consisting of integration, installation and protrusion error need to be evaluated. Due to the typically small pipe diameters, the latter may become very important [VOS96]. This results in a high measurement uncertainty when determining the integration error. On the other hand, all parameters, especially the distance from the disturbing element, can be varied freely. Laboratory measurements are not ideal to study the performance of the ADM at more than 10D distance from the element, because disturbances tend to decay faster in flow regimes with low Reynolds numbers [HAL92], yielding in too small integration errors compared to installations in power plants.

- Comparative measurements in power plants. Basically, this would be the method of choice to study integration errors. Unfortunately in most cases the ADM is compared to another primary method (i.e. current meters, thermodynamic, pressure-time) with a measurement uncertainty equal or even worse than the ADM. This makes it very often impossible to extract the total measurement error of the ADM accurately enough, not to mention the integration error, which is only a part of it.

- Numerical simulation of the ADM with CFD data. Today's CFD codes are not yet able to predict accurately turbulent flow profiles, but they are useful to understand the physical processes involved in secondary flows, which are very often not measured. Because CFD codes, which are mainly based on the k-ε closure equations, are not capable to accurately predict the decay of flow disturbances, only results for distances below 10 diameters to the disturbing element should be used for simulation calculations. The computed flow profiles will be smoother than real profiles and the peaks and depression are more pronounced. The numerical simulation of the ADM based on CFD results should therefore show a higher integration error than in real installations.
  All CFD calculations in this paper have been carried out with TASCflow™ from ASC, a software package widely used to solve fluid flow problems in the industry and in research institutes.
- Numerical simulation of the ADM with measured velocity data. By means of LDA, hotwire and pressure probe laboratory measurements the velocity distribution is measured. The acquired data is then used for simulation calculations, where the integration error is calculated as a function of the mounting angle. Current meter measurements are another possibility to obtain velocity data, if the current meters are distributed in large quantities on eight or more radii to get the necessary resolution.

The numerical simulation of the ADM with CFD and experimentally measured data has been performed with "TRIASIM", an interpolation and integration program written in "C", which is based on cubic interpolation over a triangulated area. TRIASIM handles scattered data distributions in circular and rectangular profiles and also secondary velocity components. To obtain a smooth interpolation surface, a turbulent, asymmetric velocity distribution is first fitted through the axial velocity data and then deduced before the interpolation process.

3.3 Single 90° bend

Due to centrifugal forces, the faster moving flow in the core is deflected towards the outside of the bend, displacing the slower moving flow towards the inside of the bend. These induced motions set up two cells of secondary flow, as shown in Figure 3.

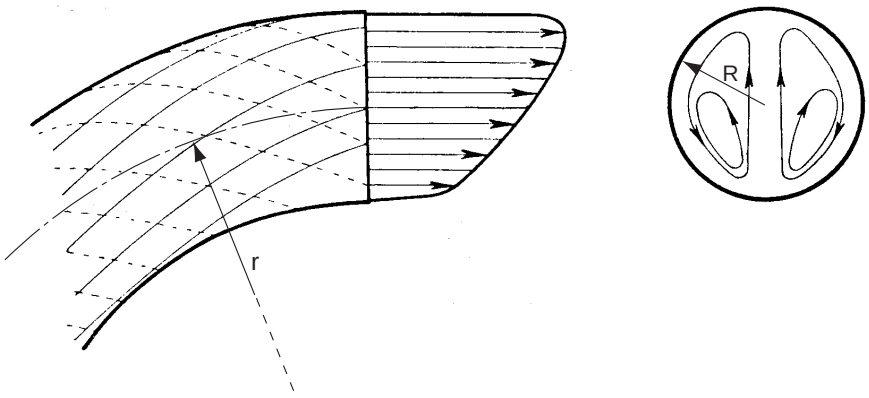

Fig.3 *Displacement of the maximum axial velocity peak and secondary flow at the outlet of a bend. Source: SCHLICHTING [SCH82]*

A flowmeter with acoustic elevation planes installed perpendicularly to the plane of the bend is not affected by the secondary flow and therefore should not need crossed paths, if the flow has not been disturbed by other disturbing elements upstream to the bend. The results from the numerical simulation presented in Figures 4 and 5 show, that this way of mounting is preferable, when only the axial velocity component is treated. First, an integration error below ±0.5% can be expected for real installations and secondly, the error curve is flat in this region, which will keep the integration error low, should the entire axial profile be rotated by ±10° due to swirl.

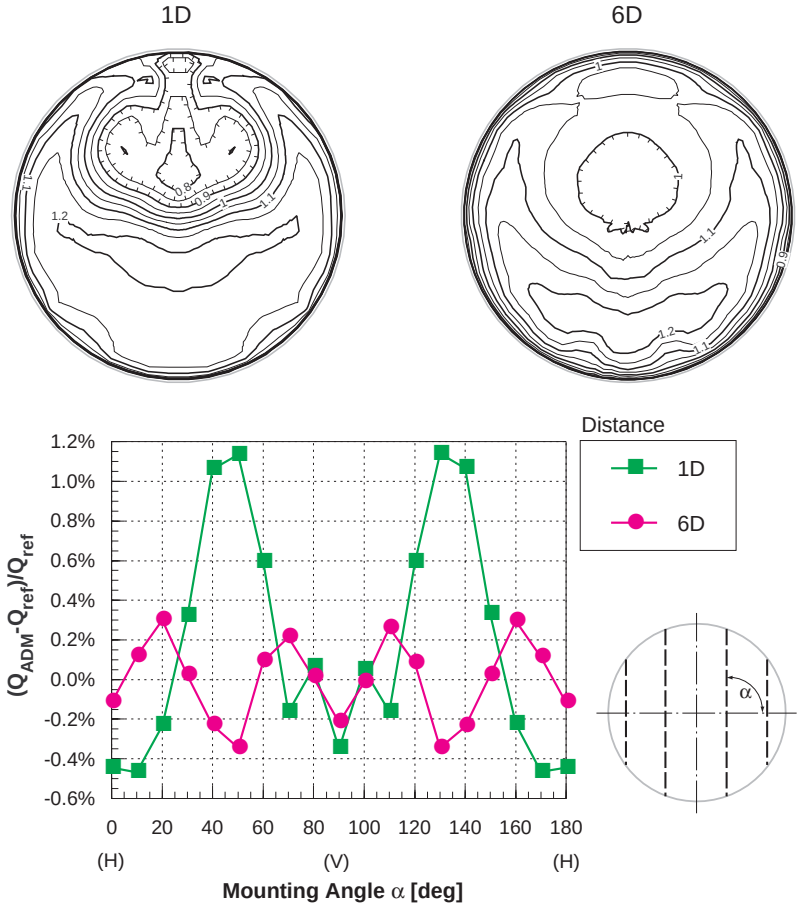

Fig.4 *<u>Above</u>: Velocity profiles measured by ENAYET et al. [ENA82] by means of LDA measurements. The parameters were R = 24 mm, the bend centerline to pipe Radius ratio r/R = 5.5 and the Reynolds number Re = 4.3·105. The flow condition at the inlet is unknown, but it is assumed to be partially developed. <u>Below</u>: Integration errors of an 8-path flowmeter, simulated with TRIASIM.*

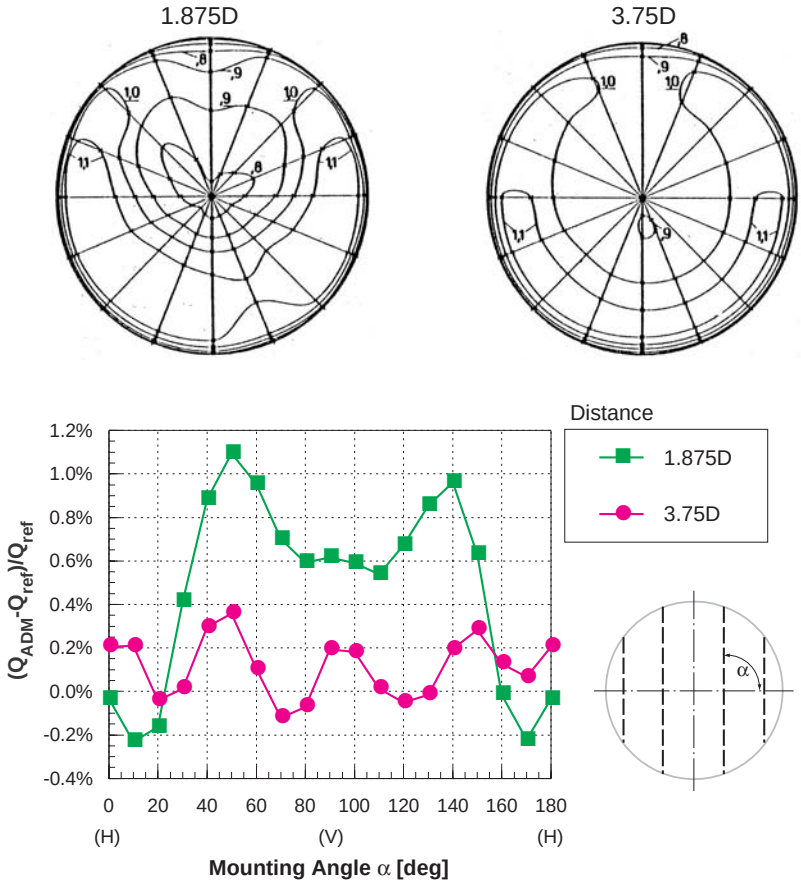

Fig.5 *<u>Above</u>: Velocity profiles measured by ETTER [ETT82] with a pitot tube. The parameters were R = 200 mm, the bend centerline to pipe Radius ratio r/R = 3, and the Reynolds number Re = 7.8·10^5. The flow profile was fully developed at the inlet of the bend. <u>Below</u>: Integration error of an 8-path flowmeter, simulated with TRIASIM.*

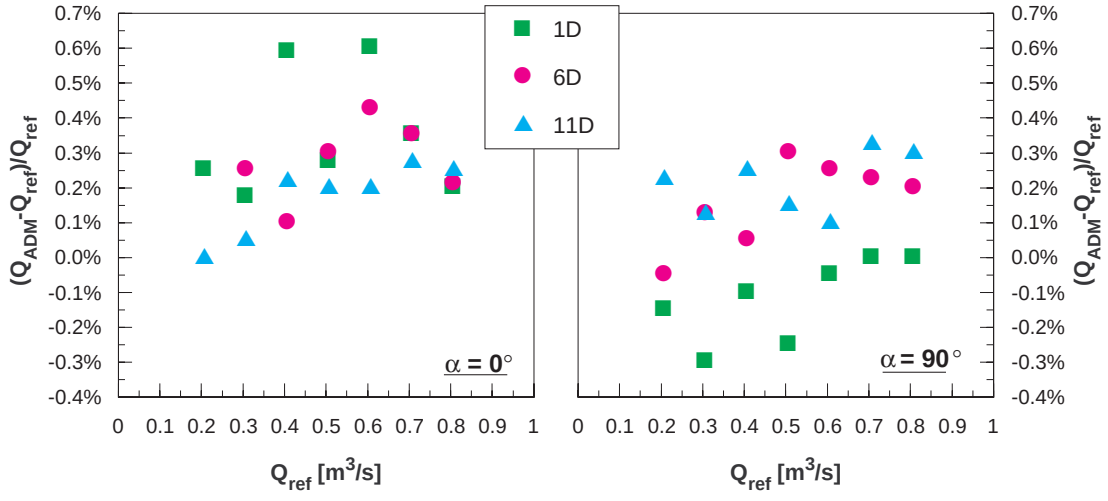

Fig.6 *Integration errors of an 8-path flowmeter behind a 90° bend measured by BRUTTIN as a function of discharge. The comparison measurements were performed at the IMHEF laboratory in Lausanne (CH) in a smooth conduit with a diameter of 450 mm. The axial flow profile at the bend inlet was only partially developed and slightly asymmetric.*

Interestingly, BRUTTIN [BRU97] has measured positive total errors behind a bend of up to +0.6% with α = 0° and lower errors for α = 90°, which is in contrast to the

results from the numerical simulation (see Figure 6). Because nonprotruding transducers were used, the difference cannot be explained by protrusion errors. However, according to BRUTTIN, the inlet profile was too flat for the given Reynolds number and slightly asymmetric. For this reason, the velocity profile at the bend outlet was possibly not typical for a 90° bend, which would explain the difference between calculated and measured integration errors. In fact, CFD calculations carried out with the same pipe and flow parameters like those of the LDA measurements from ENAYET et al. [ENA82] in Figure 4 reveal that the inlet flow profile does influence the axial velocity distribution immediately behind the bend. A fully developed and therefore more convex velocity profile at the bend inlet will result in a higher maximum velocity peak at the outlet than for the case of a partially developed, flatter inlet profile. This could have an impact on integration errors, as illustrated in Figure 7.

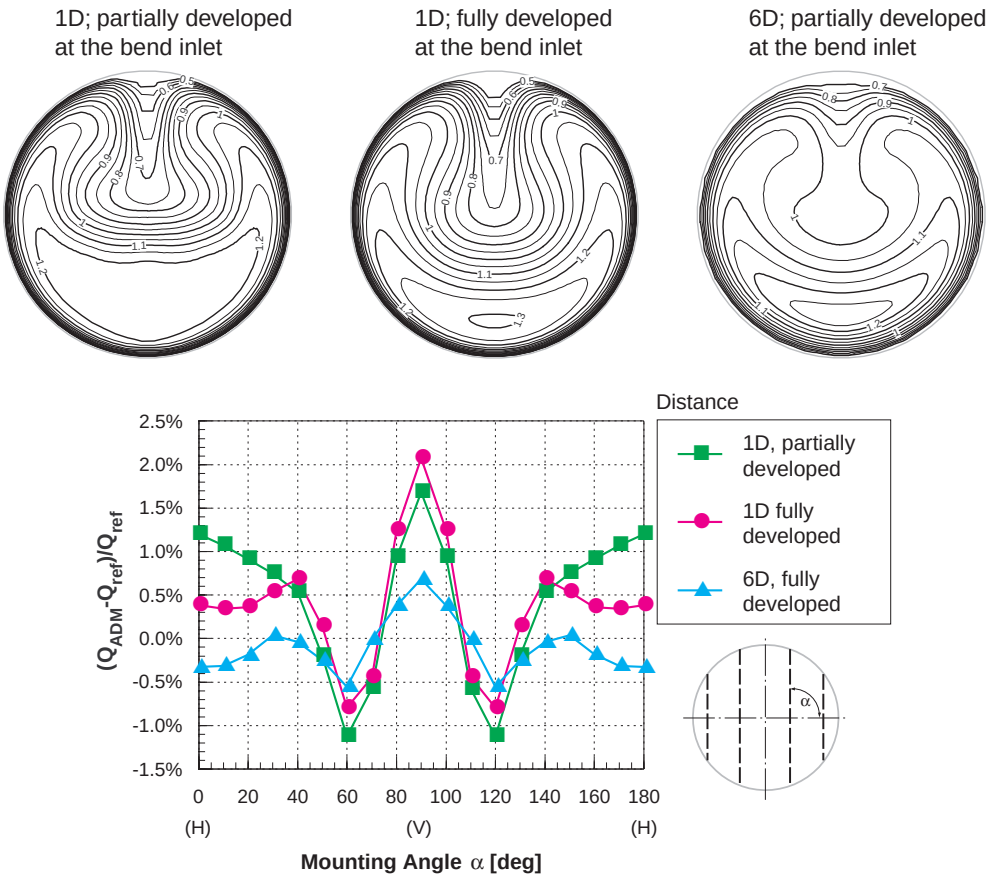

Fig.7 *<u>Above</u>: Axial velocity profiles downstream of a bend, predicted by CFD simulation for the piping configuration described in Figure 6. For the fully developed case, the straight pipe length upstream of the bend has been raised from originally 6D to 25D. <u>Below</u>: Integration error of an 8-path flowmeter, simulated with TRIASIM. Only the axial component was treated.*

As it was stated in section 3.2, the CFD calculations tend to overestimate the true integration errors. This can easily be checked by comparing the results from Figure 5 to those presented in Figure 7, where the integration errors not only seem to be to large over the full range of mounting angles, but also carry the opposite sign of the integration errors resulting from the simulation calculations. For these reasons, the results of the CFD calculation should be interpreted with great care.

3.3 Two 90°bends "out of plane" with no spacing in-between

Although piping configuration with two 90° bends and perpendicular bend planes will not be found very often in hydraulic power plants, the study of the flow characteristics and the computation of the integration error should be useful to determine upper error limits for more commonly used bend configurations with smaller bending angles and a straight pipe section in-between.

The data used for the numerical simulation calculations are from LDA measurements carried out by MATTINGLY and YEH [MAT89]. Unfortunately for the simulation calculations, the 50 measuring points were located on one vertical and one horizontal traverse, covering the inner part of the pipe cross-section area much better than the area near the wall, where much of the velocity profile has been reconstructed artificially by TRIASIM. This has definitely an adverse effect on the validity of the calculated integration errors presented in Figure 8.

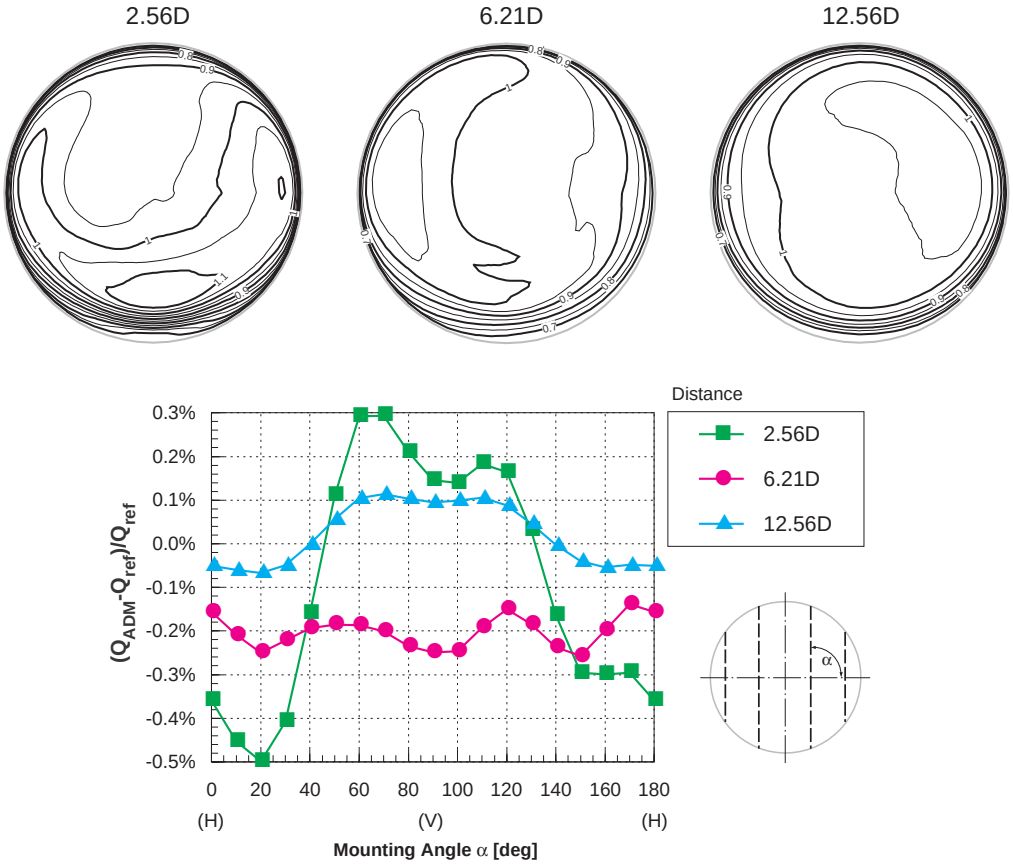

Fig.8 *Above: Velocity profiles measured by MATTINGLY [MAT89] by means of LDA measurements. The flow profile was fully developed at the inlet of the first bend; the conduit parameters are displayed in Figure 9. Below: Integration error of an 8-path flowmeter, simulated with TRIASIM.*

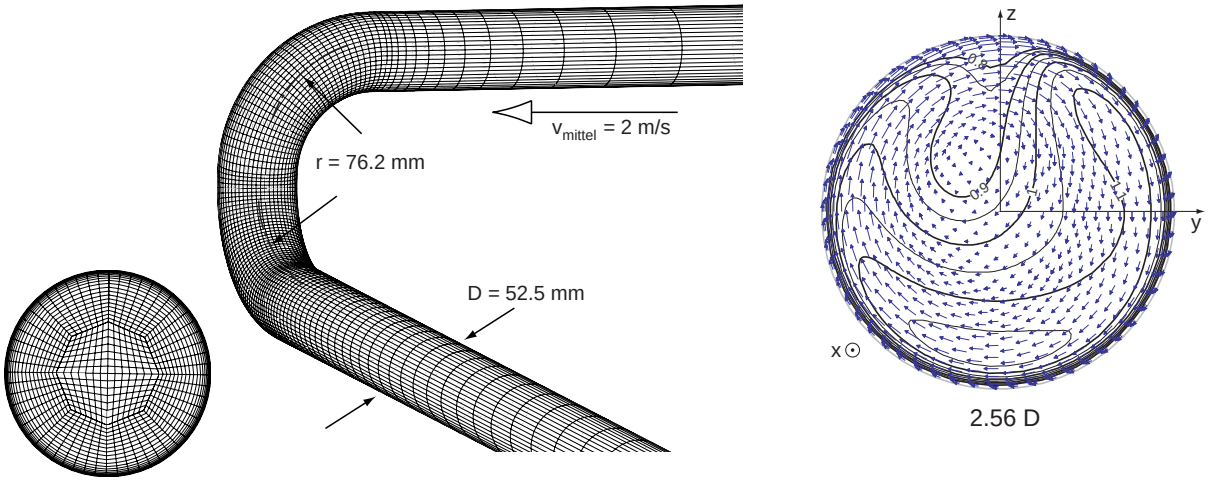

Fig.9 *Left*: Conduit geometry and CFD grid topology. The grid consisted of 260'000 grid points. *Right*: Axial velocity profile with secondary, asymmetric swirl, calculated at a distance of 2.56D downstream from the second bend.

Because no measured flow data were available immediately behind the second bend, additional CFD were carried out based on the same geometry data and flow properties than those of the LDA measurements. According to Figure 10, especially the axial velocities close to the bend and the tangential velocities are in good agreement with the measured velocities. This should result in a good prediction of the integration errors simulated with TRIASIM and the CFD data.

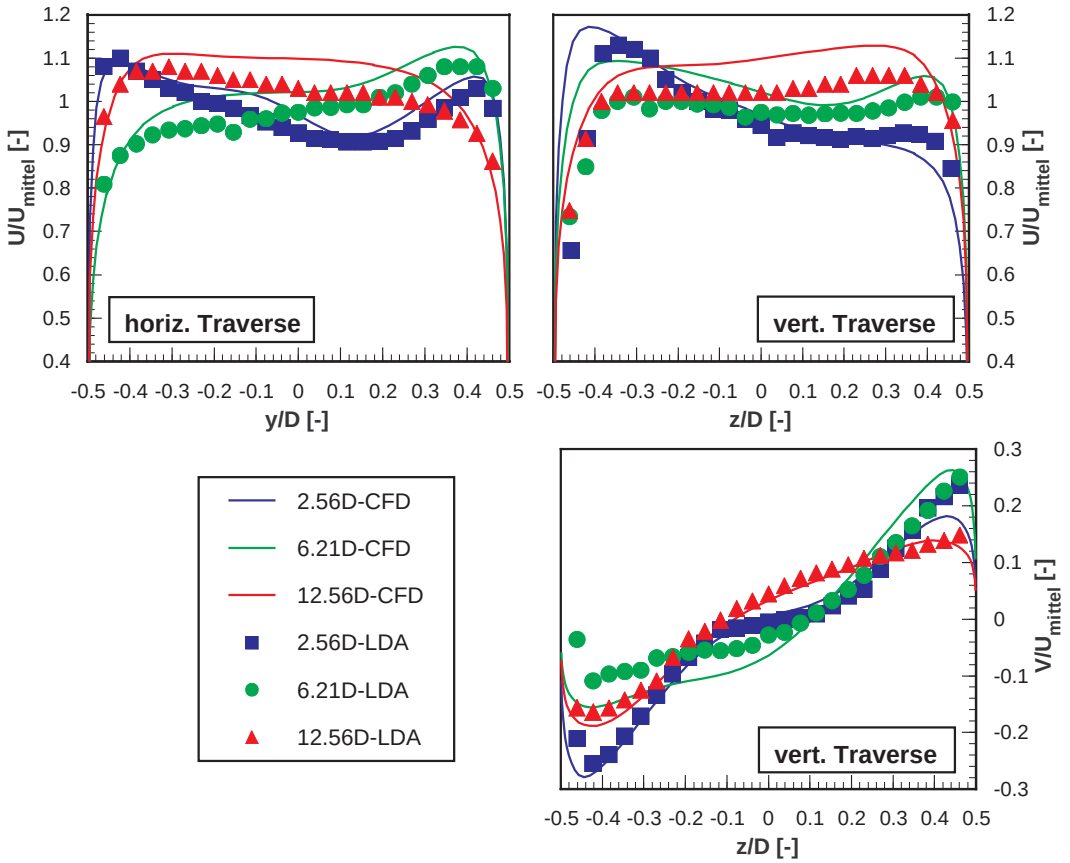

Fig.10 *Comparison between LDA measurements and CFD calculations for two bends "out of plane".*

From Figure 9 and Figure 10 it is clearly visible, that this piping configuration produces a strong asymmetric single-eddy swirl, which will rotate nearly like a solid body. This motion will persist over a very long distance, depending mainly on the friction coefficient λ, which is a function of the Reynolds number and the wall roughness. MOTTRAM [MOT86], who measured the swirl decay behind two bends "out of plane", showed that the pipe length for a decay of 50% is 10.5D for a friction factor $\lambda = 0.0046$ ($Re = 2 \cdot 10^5$, rough pipe), but for a friction factor of $\lambda = 0.0015$ ($Re = 2 \cdot 10^5$, smooth pipe) it increases to 45D. For typical Reynolds numbers found in hydraulic power plants this distance could easily reach 80D.
These flow properties are not only of academic interest, they also can have a negative impact on the flowmeter accuracy. Firstly, because of the asymmetry of the swirl (see also Fig 9), the use of crossed paths is absolutely vital for an accuracy better than ±0.5% up to distances of approximately 20D for usual Reynolds numbers and smooth pipes. This is clearly demonstrated in Figure 11, where the integration errors of a 4-path flowmeter have been compared to those of an 8-path flowmeter with crossed paths for a Reynolds number of 10^5. Secondly, according to KITO [KIT84], asymmetric swirl induces an asymmetric axial velocity distribution which will last as long as the flow is swirling. Fortunately, the distortion will no longer be severe after an estimated distance of 20D, but together with flat axial velocity distribution, which is typical for single-eddy, swirling flow, a small integration error of ±0.1% to ±0.2% will very likely remain at large distances.

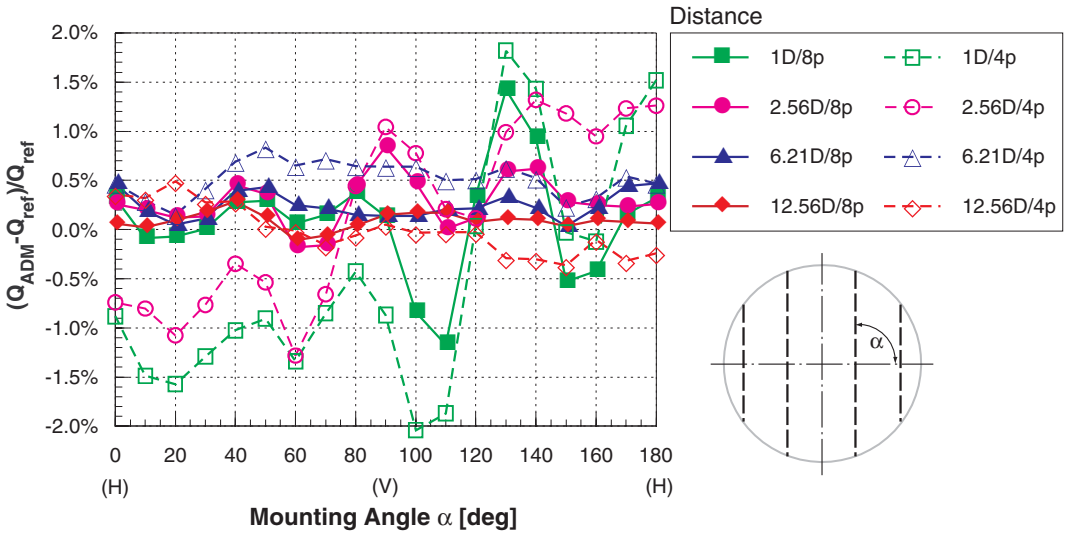

Fig.11 *Simulation of the integration error of a 4-path (1 cross-plane) and an 8-path (2 cross-planes) flowmeter based on CFD calculations. The 4-path flowmeter is influenced by the secondary flow.*

If the flowmeter is mounted immediately after the two bends, the recommended mounting position of the acoustic elevation planes is the same as for a single bend, namely perpendicular to the bend plane of the second bend. Further downstream, the axial flow, including the peaks and depressions, rotates with a varying frequency [HAL92], which will initially also depend on the bend configuration. Starting from the initially perpendicular mounting position, the acoustic paths should be rotated in with the rotation of the axial profile for a small integration error. Up to distances of 10D, CFD simulation calculations predict the rotation frequency very well and can therefore be used for determining the ideal position acoustic elevation planes.

3.4 Valves

Much too often in a hydraulic power plant, the horizontal straight pipe section, which would be ideal for an installation for an acoustic flowmeter, is already occupied by a butterfly valve. With a blockage of typically 10-20% of the cross-section area, such valves do heavily disturb the velocity profile.

To study the integration error related to these devices, we analyzed velocity measurements from ETTER [ETT82] which have been performed upstream and downstream of two different types of valves with a nominal diameter of 250mm illustrated in Figure 12 and Figure 14.

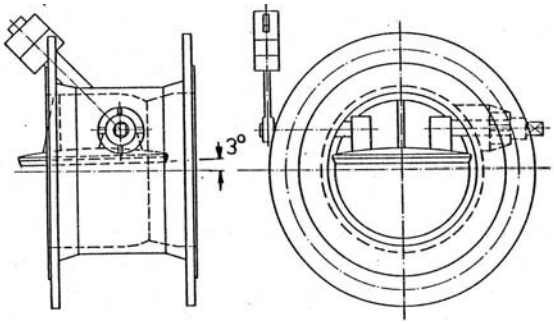

Fig.12 *Check valve with a nominal diameter of 250 mm producing velocity distributions displayed in Figure 13. Source: [ETT82].*

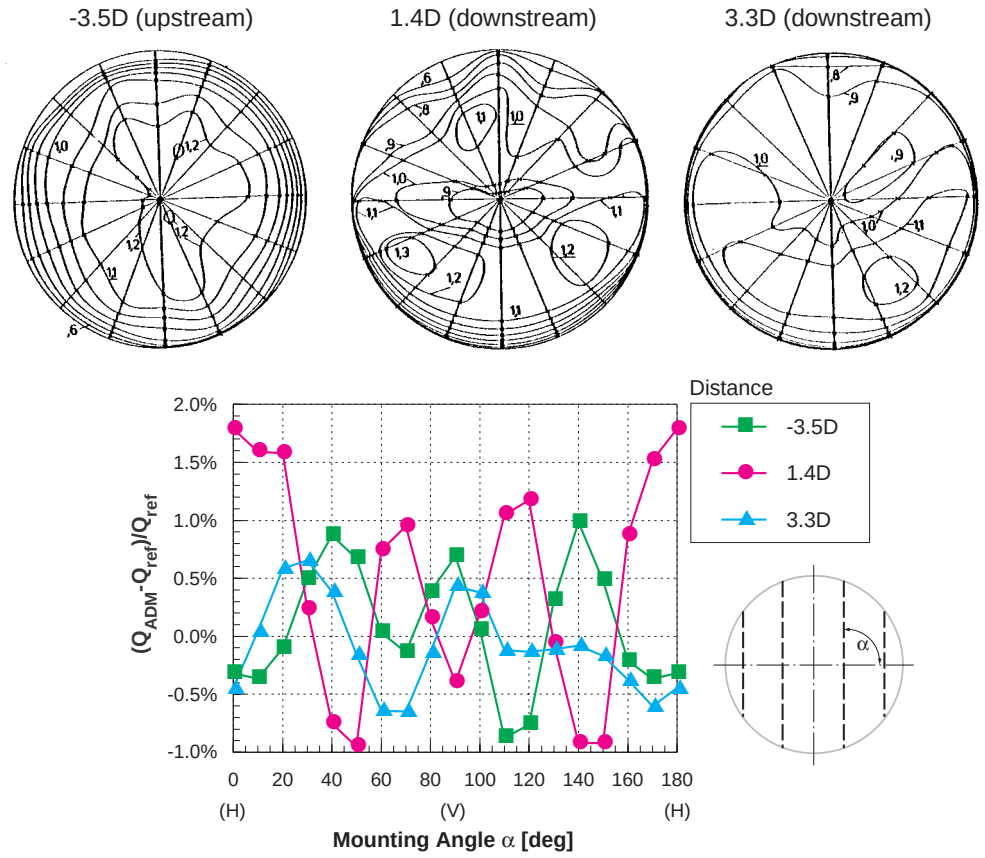

Fig.13 *<u>Above</u>: Velocity profiles produced by the check valve illustrated in Figure 12, measured by ETTER [ETT82] with a hot film probe. The parameters were R = 125 mm and the Reynolds number Re = 5·10^5. The flow profile was fully developed and the pipe hydraulic smooth. <u>Below</u>: Integration error of an 8-path flowmeter, simulated with TRIASIM.*

Of course, these two examples are far from being representative, but assuming, that valves used in larger conduits are usually more carefully designed to reduce the pressure drop, we believe, that the integration errors presented in Figure 13 and Figure 15 represent the upper range of possible errors. It is yet unclear, whether local cross-flow components, which are not neutralized by crossed paths, will evoke additional errors. Besides laboratory measurements, CFD calculations could help to clarify this open question.

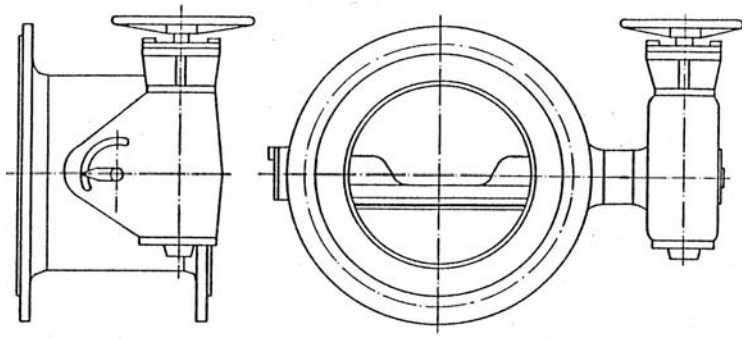

Fig.14 *Butterfly valve with a nominal diameter of 250 mm producing velocity distributions displayed in Figure 15. Source: [ETT82].*

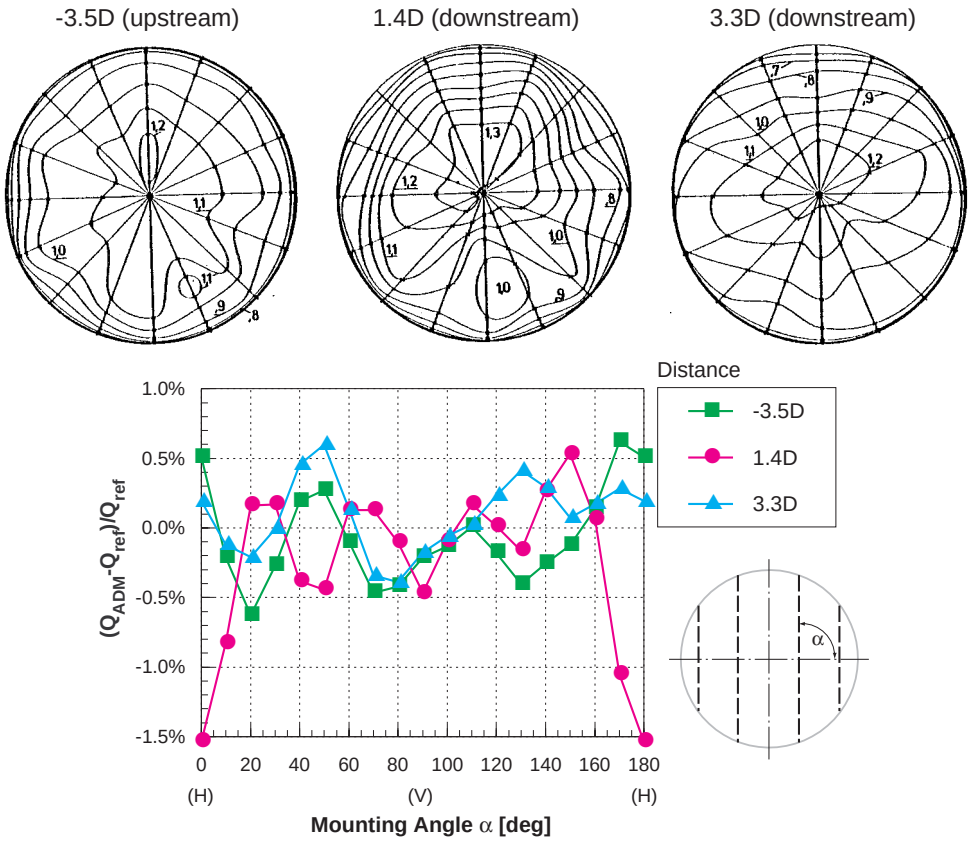

Fig.15 *<u>Above</u>: Velocity profiles produced by the butterfly valve illustrated in Figure 14, measured by ETTER [ETT82] with a hot film probe. The parameters were R = 125 mm and the Reynolds number Re = 5·10^5. The flow profile was fully developed and the pipe hydraulic smooth. <u>Below</u>: Integration error of an 8-path flowmeter, simulated with TRIASIM.*

Although it is likely, that in large pipe of power plants the integration errors will differ from the results presented above, two conclusions can be drawn:

- The orientation of the acoustic elevation planes should be perpendicular to the valve plate.
- The results indicate, that the integration error range for a flowmeter installed upstream of the valve is at least as large as for a flowmeter installed at the same distance from the valve in downstream direction.

4. Conclusion

Calculations and measurements of integration errors behind several disturbing elements illustrate, that even when the flowmeter is placed immediately behind the element, maximum integration errors will be smaller than ±1%, if the installation rules concerning the orientation of the acoustic elevation planes have been followed:

- Single bends: Orientation of the elevation planes perpendicular to the bend plane.
- Double bends with perpendicular bend planes ("out of plane"): Orientation of the elevation planes perpendicular to the second bend plane.
- Valves: Orientation of the elevation plane perpendicular to the valve plate.

In order to remain within the error limit of 1%, the OWCIS integration method, which reduces the integration error by approximately +0.15%, should be used.
Because the maximum distortion of the flow profile by a disturbing element is barely influenced by the Reynolds number, this number should hold for any Reynolds number. This is also supported by laboratory measurements from BRUTTIN [BRU97], where no Reynolds number dependency is can be detected. Due to the flatter inlet profiles, outlet profiles behind bends are flatter for higher Reynolds number. Maximum integration errors will therefore be even lower for higher Reynolds numbers in some cases. Further evidence for maximum integration errors below ±1% for Reynolds numbers of more than 10^7 has been provided by comparative measurements from GREGO in Porto Tolle (It) immediately behind a bend [GRE87] or by the calibration measurements in Pradella-Martina (CH) behind two bends, separated by dividing junction [MAN95].
At larger distances from the disturbing element, however, the integration error is influenced by the decay of the axial disturbances, which is a function of the Reynolds number and the wall roughness. For Reynolds numbers below 10^6 and for smooth conduits, the results of the numerical simulation calculations show that the integration error should be smaller than ±0.5% at a downstream distance of 5D behind the disturbing element. Because severely distorted profiles have been chosen for the simulation of the ADM, it is assumed that this error limit is valid also for disturbing elements or combinations of such elements, which have not been investigated here. For higher Reynolds numbers, the decay will be slower due to the smaller wall friction coefficient λ, which decreases with increasing Reynolds number; details of these high Reynolds number decays and its impact on acoustic discharge measurement are not fully understood and should be further investigated. According to the above statements on distorted flows the error of ±1% immediately behind a disturbing element will not be exceeded and we estimate an integration error of +-0.8% for Reynolds number above 10^7 for a distance of 5D downstream of the element.

All investigations demonstrate that the measuring position of ADM may be placed in any case closer to an upstream disturbing element than the ten conduit diameters suggested by IEC41 code.

References

BRU97 Analyse des erreurs dues à l'écoulement dans la mesure de débit par la méthode acoustique: Approches expéerimentale et numérique
Christophe Bruttin
Thèse 1746, Lausanne, EPFL, 1997 (in French)

ENA82 *Laser Doppler Measurements of Laminar and Turbulent Flow in a Pipe Bend*
M.M. Enayet, M. M. Gibson, A. M. K. P. Taylor, M. Yianneskis
Imperial College of Science an Technology, London, England, 1982

ETT82 *Bestimmung von Korrekturfaktoren für ein Ultraschalldurchflussmessverfahren in Rohrleitungen mit Störungen*
Siegbert Etter
Dissertation an der Fakultät Energietechnik der Universität Stuttgart, 1982 (in German)

GRE87 *Pipeline flowrate measurements intercomparision tests of current meters and a multipath acoustic flowmeter*
G. Grego
I.C.M.G 18th Meeting, Dubrovnik, 8 -11. Sept. 1987

HAL92 *A Model-Based Approach to Flowmeter Installation Effects*
Jouko Halttunen
Dissertation, Tampere University of Technology, 1992

KIT84 *Axi-asymmetric Character of Turbulent Swirling Flow in Circular Pipe*
O. Kito
Bulletin of the JSME 27 (1984), No. 226, p. 683-690, 1984

IEC41 *Field acceptance tests to determine the hydraulic performance of hydraulic turbines, storage pumps and pump-turbines*
International Standard CEI/IEC 41, Third Edition 1991-11

MAN95 *Kalibration der akustischen Wassermengen-Messeinrichtung im Kraftwerk Pradella-Martina*
Milof Mancal, Hans Regli, A. Voser
wasser, energie, luft, Baden, Heft 3/4, 1995 (in German)

MAT89 *Flowmeter Installation Effects - Single and Double Elbow Configurations*
G. E. Mattingly, T. T. Yeh
VDI Berichte Nr. 768 p. 65-73, 1989

MOT86 *The Swirl Damping Properties of Pipe Roughness and the Implications for Orifice Meter Installation*
R. C. Mottram, M. S. Rawat
Flow Measurement in the mid 80's, Proceedings: Volume 2, 9-12 June 1986

SCH82 *Grenzschicht-Theorie*
H. Schlichting
Verlag G. Braun, Karlsruhe 1982 (German edition)

STA96 *The Swiss National Energy Foundation Project on Acoustic Discharge Measurement*
T. Staubli, A. Voser, J.-E. Prénat, Ch. Bruttin
IGHEM Seminar, Montreal, 25.-28. Juni 1996

VOS96 *CFD-Calculations of the protrusion effect and impact on the acoustic discharge measurement accuracy*
A. Voser
IGHEM Seminar, Montreal, 25-28. Juni 1996

WAL96 *Performance of an 18 path Acoustic Flowmeter at R. Moses Niagara Power Plant Unit 13*
James T. Walsh, Peter Ludewig, Michael Hermo et al.
IGHEM Seminar, Montreal, 25-28. Juni 1996